Proline-rich polypeptide-1 decreases cancer stem cell population by targeting BAFF chromatin-remodeling complexes in human chondrosarcoma JJ012 cells

ALEXANDRA MORAN[1], AARON HOYT[1], ANIL SEDANI[1], CAROLINE GRANGER[1], SHANNON SAIGH[2], MARZENNA BLONSKA[3], LIU ZHAO-JU[4], SHEILA ANN CONWAY[1], JUAN PRETELL[1], JEFFREY BROWN[1] and KARINA GALOIAN[1]

[1]Department of Orthopaedics; [2]Flow Cytometry Core Facility, Sylvester Comprehensive Cancer Center; [3]Department of Medicine, Sylvester Comprehensive Cancer Center; [4]Department of Surgery, University of Miami, Miller School of Medicine, Miami, FL 33136, USA

Received January 29, 2020; Accepted April 8, 2020

DOI: 10.3892/or.2020.7612

Abstract. Chondrosarcoma is the second most common primary malignant bone tumor and is resistant to chemotherapy and radiation. Inadequate treatment response and poor prognosis requires novel therapeutic approaches. Proline-rich polypeptide-1 (PRP-1), synthesized by brain neurosecretory cells, has demonstrated antitumor properties in JJ012-cells; however, its underlying molecular mechanism remains unclear. The present study aimed to investigate the epigenetic regulation by which PRP-1 inhibits chondrosarcoma cancer stem cell (CSC) proliferation and to elucidate additional CSC biomarkers in human chondrosarcoma other than ALDH1A1. Human chondrosarcoma JJ012-cells were treated with PRP-1 prior to performing an Aldefluor™ assay and fluorescence-activated cell sorting in order to determine aldehyde dehydrogenase (ALDH) expression levels and isolate $ALDH^{high}$ and $ALDH^{low}$ cell populations. ALDH is an established marker of CSCs in several neoplasms, including chondrosarcoma. The cells were collected and lysed for gel electrophoresis, followed by western blot analysis. The Aldefluor™ assay was used to assess the expression levels of well-established CSC biomarkers, including CD133, CD4, CD10, CD144, CD177, CD221, CD271, leucine-rich repeat-containing G protein-coupled receptor 5, SOX2 and B lymphoma Mo-MLV insertion region 1 homolog (BMI-1), within the $ALDH^{high}$ population of JJ012 cells. The results confirmed that ALDHA1 was the biomarker for chondrosarcoma CSCs. PRP-1 was demonstrated to inhibit the $ALDH^{high}$ population colony and sarcosphere formation; 5 μg/ml PRP-1 was indicated to be the optimum concentration in eliminating colonies formed by JJ012 cells (92%, P<0.001) and by the $ALDH^{high}$ CSC-population (80.5%, P<0.001) in the clonogenic dose-response assay. Spheroid growth unequivocally decreased with an increase in PRP-1 dose. In order to determine the molecular mechanism by which PRP-1 decreased the CSC population, the regulation of the mammalian Switch/sucrose non-fermenting (SWI/SNF) complex, also referred to as BRG1-associated factor (BAF) complex, which either activates or represses transcription, thus acting as an oncogene or tumor suppressor in human cells, was analyzed. PRP-1 was demonstrated to decrease the expression levels of BRG, BAF170 and BRM; therefore, in JJ012 cells, these key players of the SWI/SNF (BAF) complex served an oncogenic role. The results of the present study demonstrated that PRP-1 targets chromatin-remodeling complexes; therefore, future efforts will be directed towards determining the interconnection between CSC maintenance, self-renewal capacity and BAF complexes.

Introduction

Bone sarcomas are a heterogenous group of different types of malignant bone tumor characterized by various degrees of mesenchymal differentiation (1). Chondrosarcoma is a rare but aggressive malignant tumor of the cells that produce the cartilage matrix; it is the third most common bone tumor, accounting for >30% of primary bone cancers in the USA, and is resistant to chemotherapy and radiation; therefore, novel therapeutic approaches are urgently required (1-4).

Cancer stem cells (CSCs) have the ability to self-renew and differentiate, which are typical characteristics of any stem cell (5). It has been reported that a tumor contains different stem cell-like populations due to decreased cell differentiation within a tumor, and this heterogenous population includes CSCs (5). DNA damage may render tissue stem cells to become CSCs during the process of differentiation and to accumulate to form different types of tumor (6). Increasing evidence suggests that CSCs exist as a sub-population of quiescent

Correspondence to: Dr Karina Galoian, Department of Orthopaedics, University of Miami, Miller School of Medicine, 1600 NW 10th Avenue, Miami, FL 33136, USA
E-mail: kgaloian@med.miami.edu

Key words: chondrosarcoma, cancer stem cells, aldehyde dehydrogenase, proline-rich polypeptide-1

cells within the dominant tumor bulk of heterogeneous tumor cells. These typically dormant cells are resistant to standard antitumor therapies such as chemotherapy and radiation, and they appear capable of self-renewal and differentiation, which suggests that CSCs are responsible for tumor repopulation following removal of the bulk tumor (7-9).

Proline-rich polypeptide-1 (PRP-1), also termed galarmin, is synthesized by the brain neurosecretory cells and comprises 15 amino acids (10). PRP-1 is an mTOR kinase (mTORC1) inhibitor in chondrosarcoma that inhibits cell proliferation (11). Furthermore, PRP-1 has been demonstrated to upregulate several tumor suppressors of the desmosomal protein family, such as desmoglein, and plakoglobin (12), as well as tumor suppressors involved in inflammatory pathways (13) and microRNAs (miRNAs), and to downregulate onco-miRNAs in the human chondrosarcoma JJ012 cell line through inhibition of mTORC1 (3,14). PRP-1 also serves an antiproliferative role via downregulation of the embryonic stem cell marker, miRNA (miR)-302-c and its targets nanog homeobox (NANOG), c-Myc and polycomb protein B lymphoma Mo-MLV insertion region 1 homolog (BMI-1) (3). Pattern recognition receptors of the adaptive immune system, including Toll-like receptor 1 (TLR1), TLR2, TLR6 and secreted mucin 5B, have been recently identified as binding partners for PRP-1, resulting in tumor suppressive effects (4). PRP-1-treated cells have been demonstrated to accumulate in the S phase, thus delaying cell cycle progression (15). The cytostatic, antiproliferative, immunomodulatory and tumor suppressive roles of PRP-1 indicate its potential as a therapeutic agent against human chondrosarcoma cells resistant to radiation and chemotherapy (3,4,10-12,14). The aforementioned properties were further investigated in the present study to determine the ability of PRP-1 to target chondrosarcoma CSCs.

Aldehyde dehydrogenase (ALDH) is an established marker of CSCs in several neoplasms. Cells expressing high levels of ALDH have been isolated in a number of human sarcoma cell lines, including the human chondrosarcoma SW-1353 cell line (16). Identification of normal and malignant stem/progenitor cells by the same marker reinforces the concept that stem and progenitor cells are primary targets of transformation, which further supports the CSC hypothesis. Furthermore, the ability to identify stem/progenitor cells by ALDH1 expression permits analysis of cancer initiation and progression from the normal to the pre-malignant and the malignant states (2,17). A widely accepted method for identifying CSCs is based on detecting the enzymatic activity of ALDH1, a detoxifying enzyme responsible for the oxidation of intracellular aldehydes (16). The self-renewal capacity, proliferative and metastatic roles of ALDH demonstrate its potential as a therapeutic target against human chondrosarcoma (18).

The present study aimed to determine the underlying molecular mechanism by which PRP-1 decreases the CSC population, with particular focus on the mammalian Switch/sucrose non fermentable (SWI/SNF)-complex (19), which can either activate or repress transcription, and to identify additional biomarkers for chondrosarcoma.

Materials and methods

Tissue culture. The human JJ012 chondrosarcoma cells were obtained from Dr Joel Block's Laboratory (Rush University, Chicago, USA). The cells were maintained in complete growth medium containing DMEM + GlutaMAX™ supplemented with F-12 + GlutaMAX™ Nutrient mixture (Ham) (Thermo Fisher Scientific, Inc.), 10% FBS (Sigma-Aldrich; Merck KGaA), 1% penicillin/streptomycin (Thermo Fisher Scientific, Inc.), 25 μg/ml ascorbic acid, 100 ng/ml insulin and 100 nM hydrocortisone (Sigma-Aldrich; Merck KGaA). The cells were incubated at 37˚C in a humidified atmosphere with 5% CO_2 and periodically checked for mycoplasma. Estrogen negative MDA-MB-231 breast cancer cells (ATCC® CRM-HTB-26) were obtained from ATCC. The medium for this cell line was ATCC-formulated Leibovitz's L-15 Medium (cat. no. 30-2008; ATCC) supplemented with 10% FBS. The MDA-MB-231 breast cancer cells were incubated at 37˚C in a humidified atmosphere with 5% CO_2. Human B cell lymphoma (HT; cat. no. ACC567), Ly1 (cat. no. ACC722) and Ly3 (cat. no. ACC761) cell lines were obtained from DSMZ. Ly10 cells were a gift from Dr Messner (Ontario Cancer Institute, Canada), and HBL-1 cells were a gift from Dr Vega (MD Anderson Cancer Center, Houston, TX, USA). Melanoma metastatic cell line C81618 was provided by Dr Liu, University of Miami, Miller school of Medicine.

Mycoplasma detection assay. JJ012 chondrosarcoma cells were seeded 1x10^5 cells/ml in full growth media and treated with 25 μg/ml Plasmocin™ (InvivoGen) for 14 days. Plasmocin™-containing medium was replaced every 3-4 days. MycoAlert® Mycoplasma Detection kit (cat. no. LT07-118; lot. no. 0000678423; Lonza, Inc.) was used according to the manufacturer's instructions. The microplate was placed in the Molecular devices Spectra Max microplate luminometer (Lonza, Inc.) and programmed for Reading A analysis. A total of 100 μl MycoAlert™ substrate was added to each sample and incubated for 10 min, following which the luminometer was programmed for Reading B analysis, and the Reading B/Reading A ratio was calculated.

Cell viability. Cells were cultured under the same conditions as previously described and stained with 0.4% trypan blue stain (Gibco; Thermo Fisher Scientific, Inc.) at a 1:1 ratio. After a 72-h incubation at 37˚C in the 5% CO_2 incubator, cells were observed using the Luna II Automated Cell Counter™ (Logos Biosystem) according to the manufacturer's protocol to generate cell count and viability data.

PRP-1 treatment. A subset of cultured human JJ012 chondrosarcoma cells were treated with 10 μg/ml PRP-1 as previously described (10) and incubated at 37˚C in a humidified atmosphere of 5% CO_2 for 24 h prior to performing the Aldefluor™ assay. Cell proliferation was measured in cells seeded at 5x10^4 cells/ml using the Rapid Cell Proliferation kit (EMD Millipore), according to the manufacturer's instructions.

Aldefluor™ assay and fluorescence-activated cell sorting (FACS). The Aldefluor™ assay (StemCell Technologies, Inc.) was performed according to the manufacturer's protocol, in order to detect cells with ALDH activity. Briefly, the JJ012 cells were harvested and resuspended in Aldefluor™ assay buffer at a density of 1x10^6/ml. The cells were incubated with 25 μl DMSO with 25 μl 2N HCl for 15 min, followed by addition of 360 μl

assay buffer in order to activate the Aldefluor™ reagent, and incubated for 45 min at 37˚C. N,N-Diethylaminobenzaldehyde (DEAB), a specific ALDH inhibitor, was used as the negative control. Following incubation, all tubes were centrifuged for 5 min at 250 x g at 4˚C, the supernatant was discarded and the cells were resuspended in Aldefluor™ assay buffer. The cells were then transferred to 5 ml Falcon polystyrene round bottom tubes with cell strainer caps. After labeling, the samples with and without PRP-1 treatment were sorted using a FACSAria II flow cytometer (BD Biosciences) with FACSDiva software (version 6.1.3; BD Biosciences) into $ALDH^{low}$ and $ALDH^{high}$ cells. Data analysis was performed using FlowJo software (version 10; FlowJo, LLC).

Gel electrophoresis and western blotting. Chondrosarcoma JJ012 cells were cultured to 100% confluency. Cells were collected using trypsin, seeded into petri dishes at a density of $1x10^6$ cells/ml and incubated for 24 h at 37˚C in a 5% CO_2 incubator. After 24 h, cells were washed with ice-cold PBS, and protease inhibitor was added to the CelLytic M cell lysis reagent (Sigma-Aldrich; Merck KGaA) at a 1:100 ratio, and kept in a 5% CO_2 incubator for 10 min. Following collection of cells with a rubber scraper and cell membrane lysis with an 18-gauge needle, the cells were centrifuged at 15,000 x g at 4˚C for 10 min. The supernatant was collected, and the protein content was measured using a NanoDrop® spectrophotometer. The supernatant was frozen at -80˚C until loading into gels (20 μg/lane). Polyacrylamide gel electrophoresis and western blotting reagents were supplied by Lonza Group, Ltd., and the experiments were performed according to the manufacturer's protocols. The reagents used were as follows: Pager Gold Precast Gels (10% Tris-Glycine; Lonza Group, Ltd.); ProSieve Quad Color Protein marker (4.6-300 kD; Lonza Group, Ltd.); 20X reducing agent for ProSieve ProTrack Dual Color Loading buffer (Lonza Group, Ltd.); ProTrack Loading buffer (Lonza Group, Ltd.); ProSieve ProTrack Dual Color Loading buffer EX running buffer (Lonza Group, Ltd.); ProSieve EX Western Blot Transfer buffer (Lonza Group, Ltd.) and Immobilon®-P Polyvinylidene difluoride membranes (Sigma-Aldrich; Merck KGaA).

For the blocking step, Western Blocker solution (Sigma-Aldrich; Merck KGaA) was used. Primary antibodies were diluted in blocking buffer at the ratio of 1:1,000, and the membranes were incubated at 4˚C overnight with gentle agitation. The secondary antibodies horseradish peroxidase-conjugated goat anti-rabbit IgG (cat. no. A0545; Sigma-Aldrich; Merck KGaA) and anti-mouse IgG (cat. no. A4416; Sigma-Aldrich; Merck KGaA) were diluted to 1:5,000, and the membranes were incubated for 2 h at room temperature with gentle agitation. Western blot visualization was performed using ECL reagents (GE Healthcare Life Sciences) for 1 h at room temperature.

Antibodies for western blotting. The primary antibodies used for western blot analysis were as follows: CD133 (cat. no. 19898; Abcam), CD144 (VE-cadherin) monoclonal (16B1) PE-Cyanine7 (cat. no. 25-1449-4; Invitrogen; Thermo Fisher Scientific, Inc.), c-Kit (Ab 81) (cat. no. 13508; Santa Cruz Biotechnology, Inc.), rabbit LGR5 (GPR49) (cat. no. 9205024; MyBioSource, Inc.), SOX2 (cat. no. 97959; Abcam), human ALDH1A1 (cat. no. MAB5869; R&D Systems, Inc.), polycomb complex protein oncogene BMI-1 (BMI-1; cat. no. 38295; Abcam), c-Myc (9E10) (cat. no. 40; Santa Cruz Biotechnology, Inc.), CD44 (cat. no. 6124; Abcam), FOXO3 (cat. no. MAB6165; R&D Systems), FOXC1 (cat. no. MAB 6329; R&D Systems), NANOG clone 7F7.1 (cat. no. MABD24; Sigma-Aldrich; Merck KGaA), anti CD34 + mesenchymal stem cell monoclonal antbody (STRO-1; cat. no. 39-8401; Thermo Fisher Scientific, Inc.), CD117 c-Kit (Ab 81) (cat. no. 13508; Santa Cruz Biotechnology, Inc.), BRG1-associated factor 170 (BAF170) or SMARCC2 (cat. no. 9401447; MyBioSource, Inc.), BRG1-associated factor 155 (BAF155) or SMARCC1 (cat. no. 8245507; MyBioSource, Inc.), protein Brahma homolog 1 (BRG1; cat. no. 4081; Abcam), Brahma protein (BRM) or SMARCA 2 (cat. no. 610390; BD Biosciences), ARF tumor suppressor, p14ARF antibody (ARF 4C6/4; cat. no. 53392; Santa Cruz Biotechnology, Inc.), cyclin-dependent kinase inhibitor 2A (CDKN2A) P15/P16 (p15, INK4b; p16, INK4a; cat. no. 377412; Santa Cruz Biotechnology, Inc.), p-topoisomerase IIα (TOP2A) (Ser1469) (cat. no. 13072; Cell Signaling Technology, Inc.), tubulin (cat. no. T5168; Sigma Aldrich; Merck KGaA) and topoisomerase IIα SER1469 [cat. no. 13072 (E); Cell Signaling Technology, Inc.].

Densitometry analysis of western blots. Quantitative analysis and densitometry were obtained using integrated density analysis on ImageJ software 1.52e (National Institutes of Health) to calculate relative optical density (OD) of the previously mentioned proteins compared with the housekeeping protein tubulin; the bulk untreated JJ012 was used as the control.

Apoptosis assay and cell cycle analysis. Staining was performed using the Annexin V Apoptosis Detection kit according to the manufacturer's protocol. Modified Annexin V/propidium iodide (PI) apoptosis assay (cat. no. 88-8007-72; eBioscience; Thermo Fisher Scientific, Inc.) was used for apoptosis experiments with $1x10^6$ cellss/ml. The LRS-II Analyzer was used with DiVa-8 software (BD Biosciences). The antibodies used for flow cytometric analysis were as follows: APC-conjugated human CD133 (cat. no. FAB11331A-025; R&D Systems, Inc.), Alexa Fluor® 647 mouse anti-human BMI-1 clone P51-311 (cat. no. 562637; BD Biosciences), CD144 (VE-cadherin) (16B1) phycoerythrin (PE)-cyanine7 (cat. no. 25-1449-4; Invitrogen; Thermo Fisher Scientific), BV605 mouse anti-human CD117 clone 104D2 (cat. no. 562687; BD Biosciences), PE-CF594 rat anti-human LGR5 (N-terminal) clone 8F2 (cat. no. 563470; BD Biosciences), PE mouse anti-SOX2 clone 245610 (cat. no. 560291; BD Biosciences), BV421 mouse anti-human CD49b (cat. no. 564119; BD Biosciences), CD10 (SN5c) PerCP-eFluor 710 (cat. no. 46-0108-41; Invitrogen; Thermo Fisher Scientific, Inc.), PE-CF594 mouse anti-human CD221 clone 1H7 (cat. no. 562535; BD Biosciences) and Alexa Fluor® 647 mouse anti-human CD271 clone C40-1457 (cat. no. 560326; BD Biosciences).

Aldefluor™ assay and fluorescence-activated cell sorting (FACS). To measure cells with ALDH activity, the Aldefluor™ assay (cat. no. 01700; StemCell Technologies, Inc.) was performed according to manufacturer's protocol. Briefly, cells were harvested and resuspended in Aldefluor™ assay buffer at

a density of $1x10^6$ cells/ml. To activate the Aldefluor™ reagent, first 25 μl DMSO was added and incubated for 15 min with 25 μl 2N HCl, and then 360 μl assay buffer was added to the vial. The cells were incubated with the activated Aldefluor™ reagent for 45 min at 37˚C. Diethylaminobenzaldehyde (DEAB), a specific ALDH inhibitor, was added as a negative control. Following incubation, all tubes were centrifuged for 5 min at 250 x g, at 4˚C and the supernatant was removed; the cells were then resuspended in Aldefluor™ assay buffer, transferred and strained into a Falcon 5 ml polystyrene round bottom tube with a cell strainer cap (cat. no. 352235; Thermo Fisher Scientific, Inc.). After labeling, the samples were sorted using a Special Order Research Product (SORP) FACSAria II (BD Biosciences) using BD FACSDiva software (version 6.1.3; BD Biosciences) into $ALDH^{low}$ and $ALDH^{high}$ cells with and without PRP-1 treatment. Data analysis was performed using FlowJo software version 10 (FlowJo LLC).

Bromodomain-containing protein 4 (BRD4) inhibitor screening. The cells were seeded at 4,000 cells/well in 384-well plates. BRD4 inhibitor screening was performed by BPS Bioscience Inc., using the BPS Bioscience TR-FRET Assay kit BRD4 according to the manufacturer's instructions.

Statistical analysis. All statistical analyses were performed using GraphPad Prism (version 8.0.2; GraphPad Software, Inc.). Statistical analyses were performed using individual unpaired t-tests for flow cytometry experiments (repeated 10 times). Statistical analyses of relative ODs were completed using one-way ANOVA, followed by Tukey's or Dunnett's post hoc multiple comparison test, and the data were expressed as 95% confidence intervals of the mean difference. All western blots were performed in triplicate. $P<0.05$ was considered to indicate a statistically significant difference. Data are presented as the mean ± standard error of the mean in all graphs with $^{*}P<0.05$, $^{**}P<0.01$ and $^{***}P<0.001$.

Results

The inhibitory action of PRP-1 is disease-specific. It has previously been reported that PRP-1 displays disease-specific inhibition of tumor growth; however, in chondrosarcoma, PRP-1 inhibits the stemness signature cluster of miR-302-367 (3). For example, in glioblastoma, miR-302-367 is strongly induced during serum-mediated stemness suppression, which prevents PRP-1 from exerting inhibitory effects on tumor cell proliferation (3). Thus, the present study assessed different types of malignancies, such as lymphoma and melanoma.

PRP-1 failed to inhibit the growth of two major subtypes of diffuse large B-cell lymphoma: Activated B-cell subtype lymphoma 3, 10 (Ly3, Ly10), human B line (HBL1) and germinal center subtype (Ly1 and HT cell lines). The results also demonstrated that proliferation of the metastatic melanoma cell line C81618 was not inhibited by PRP-1. The effect of PRP-1 on cell proliferation was assessed *in vitro* (data not shown).

ALDH1A1 is be the only biomarker for CSC population in human chondrosarcoma JJ012 cell line. In order to identify additional biomarkers for chondrosarcoma CSCs in the JJ012 cell line, two different approaches were employed, the traditional side population (SP) approach and the enzymatic ALDH1A1 approach. The SP analysis results demonstrated that no SPs for JJ012 cells were detected (data not shown) despite previous reports of successful identification of SP in sarcomas (20). Subsequently, known biomarkers of different types of cancer were assessed using the human chondrosarcoma JJ012 cell line. A number of well-known markers and the Aldefluor assay were employed in order to determine ALDH expression in human chondrosarcoma JJ012 cells, with and without PRP-1 treatment, and the cells were divided into $ALDH^{low}$ and $ALDH^{high}$ populations, respectively.

Human chondrosarcoma JJ012 cells were stained with Aldefluor™ in the presence and absence of the ALDH inhibitor DEAB. The DEAB (+) group was used to determine $ALDH^{low}$ and $ALDH^{high}$ populations (Fig. 1A). JJ012 fractions treated with PRP-1 were labeled as $ALDH^{low\text{-}PRP\text{-}1}$ (21). These gates were used in the analysis of surface staining of well-established CSC markers for sarcoma. Similar to the control MDA-MB-231 breast cancer cells, JJ012 cells expressed CD133, a known CSC marker (22-25). However, no difference was observed in CD133 expression between the $ALDH^{high}$ and $ALDH^{low}$ groups (Fig. 1B). The cells were stained with other surface antibodies that also demonstrated no difference in the expression levels of BMI-1, SOX2, CD144, CD117, CD221, LGR5, CD271, CD10 and CD49b between the $ALDH^{high}$ and $ALDH^{low}$ cells (Fig. 1C). Thus, none of the aforementioned markers could serve as a CSC marker.

Western blot analysis demonstrated decreased expression levels of BMI, c-Myc and NANOG in the $ALDH^{low\text{-}PRP\text{-}1}$ fraction following treatment with PRP-1 compared with untreated $ALDH^{low}$ and $ALDH^{high}$ fractions (Fig. 1D). However, no differences in the expression levels of CD44, FOX03 and FOXC1 were demonstrated between the fractions. Of note, compared with that in the $ALDH^{low\text{-}untreated}$ group, the expression of SOX2 stemness-associated factor in cancer was upregulated in $ALDH^{high\text{-}untreated}$ and $ALDH^{low\text{-}PRP\text{-}1}$, and was downregulated in the $ALDH^{low\text{ -}untreated}$ fraction (Fig. 1E). Individual one-way ANOVA of the protein markers demonstrated significant differences between $ALDH^{low\text{-}untreated}$, $ALDH^{high\text{-}untreated}$ and $ALDH^{low\text{-}PRP\text{-}1}$ cells in the expression levels of BMI-1, NANOG, LGR5, SOX2, c-Myc and FOXC1 (Table SI). No differences of means between the groups were detected for FOXO3. $ALDH^{low\text{-}PRP\text{-}1}$ cells exhibited a significantly lower BMI-1 expression level compared with $ALDH^{high\text{-}untreated}$ cells. Furthermore, NANOG expression was significantly lower in $ALDH^{low\text{-}PRP\text{-}1}$ cells compared with $ALDH^{low\text{-}untreated}$ and $ALDH^{high\text{-}untreated}$ cells. $ALDH^{high\text{-}untreated}$ cells and $ALDH^{low\text{-}PRP\text{-}1}$ cells had significantly lower expression levels of LGR5 compared with $ALDH^{low\text{-}untreated}$ cells (Fig. 1E).

In a JJ012 bulk untreated subpopulation, 4.2% untreated cells were $ALDH^{low}$ and 42.9% $ALDH^{high}$ (Fig. 2A), whereas a PRP-1-treated subpopulation demonstrated a notable change in $ALDH^{low\text{-}PRP\text{-}1}$ (82.6%) and $ALDH^{high\text{-}PRP\text{-}1}$ (0.6%) cells (Fig. 2B). Fig. 2A demonstrates one of the 10 representative experiments of the untreated JJ012 cells, whereas Fig. 2B shows one of the 10 representative experiments of the PRP-1 treated JJ012 cells; Fig. 2C is the average of the 10 experiments with the SEM represented. The individual results are presented to demonstrate how

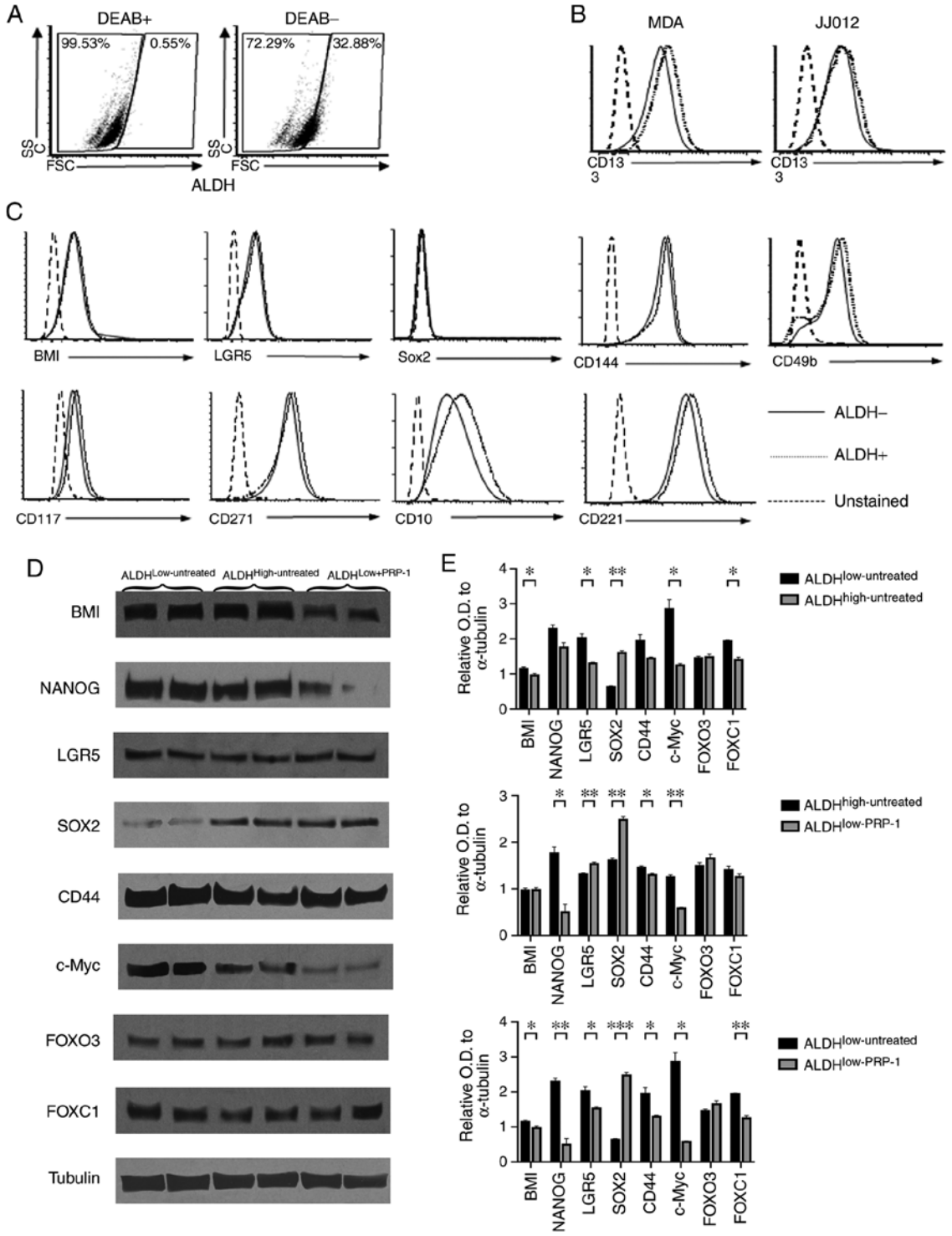

Figure 1. Identification of additional biomarkers for human chondrosarcoma. (A-C) Flow cytometry experiments. (A) The DEAB (+) group was used to determine ALDH^{low} and ALDH^{high} populations. (B) CD133 was not different between the two populations. (C) Staining with BMI-1, SOX2, CD144,CD117, CD221, LGR5, CD271, CD10 and CD49b on ALDH^{high} and ALDH^{low} cells verified that none of them was a biomarker for JJ012 human chondrosarcoma cells. (D) Western blot analysis of LGR5, SOX2, CD44, FOX03, FOXC1, BMI-1, c-Myc and NANOG. Only BMI-1, c-Myc and NANOG in ALDH$^{low+PRP-1}$ exhibited decreases in protein expression expression compared with that in ALDH^{low} and ALDH^{high} untreated cells. (E) Histograms of the relative OD in ALDH fractions. *P<0.05, **P<0.01 and ***P<0.001. ALDH, aldehyde dehydrogenase; OD, optical density; BMI-1, B lymphoma Mo-MLV insertion region 1 homolog; NANOG, nanog homeobox; LGR5, leucine-rich repeat-containing G protein-coupled receptor 5; FOXO3, forkhead box O3; FOXC1, forkhead box C1; DEAB, N,N-diethylaminobenzaldehyde.

the gating was performed by the flow cytometry software. The mean value for ALDH$^{low-untreated}$ cells was 45.03% vs. 87.53% for ALDH$^{low-PRP-1}$ treated cells. The mean value for ALDH$^{high-untreated}$ was 46.72% vs. 8.27% for ALDH$^{high-PRP-1}$ treated cells (Fig. 2C; Table SII). Subpopulations were collected using flow cytometry and consisted of the following; ALDH^{high} cells sorted from untreated JJ012 (ALDH$^{high-untreated}$), ALDH^{low} cells sorted from untreated JJ012 (ALDH$^{low-untreated}$) and ALDH^{low} cells sorted from PRP-1-treated JJ012 (ALDH$^{low-PRP-1}$). ALDH^{high} cells from

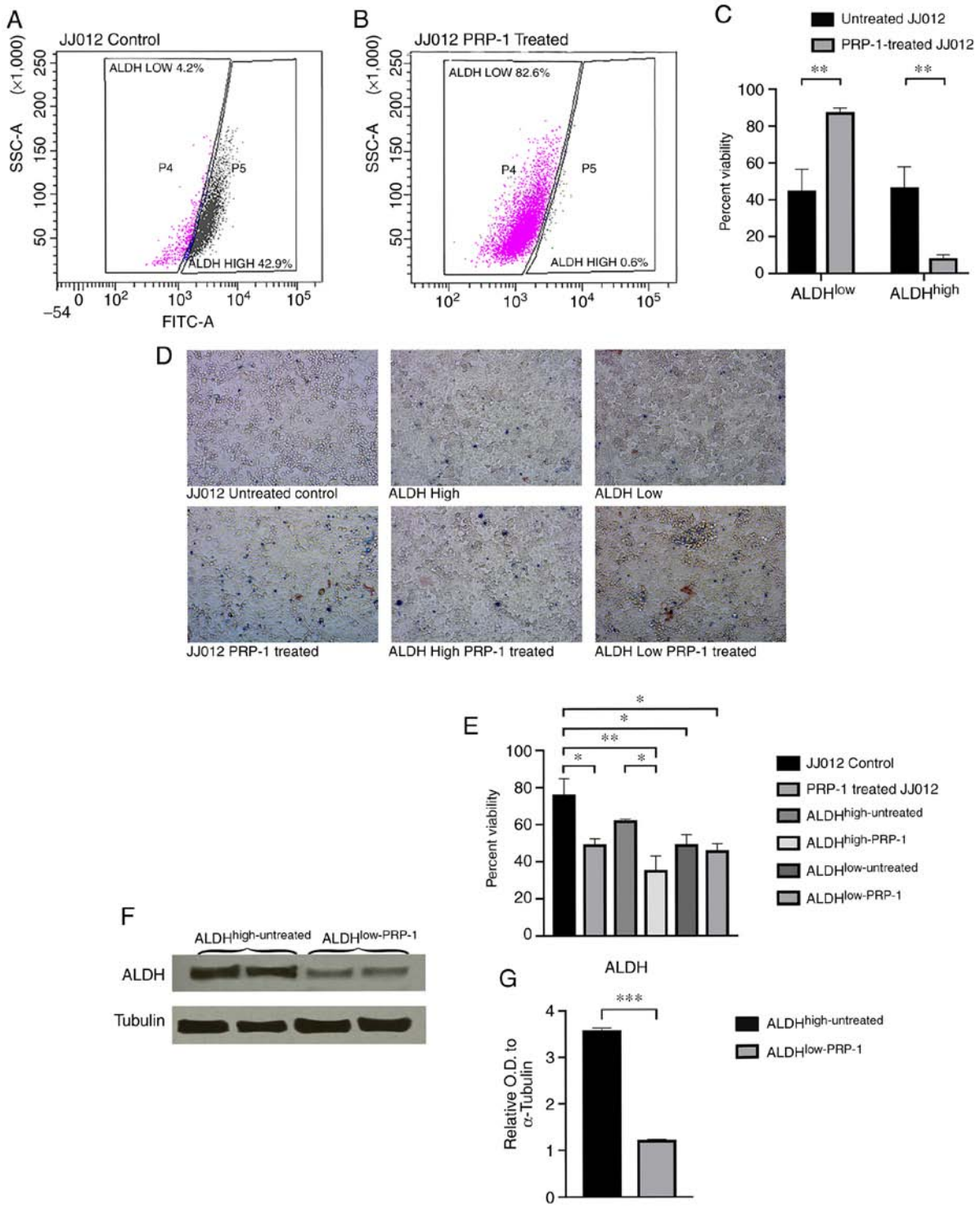

Figure 2. Flow cytometry data of JJ012 untreated and PRP-1 treated subpopulations. (A and B) Notable changes were observed between (A) $ALDH^{low}$ 4.2% and $ALDH^{high}$ 42.9% in the untreated populations and (B) 82.6% in $ALDH^{low\text{-}PRP\text{-}1}$ and 0.6% in $ALDH^{high\text{-}PRP\text{-}1}$. Panel A demonstrates one of the 10 representative experiments of the untreated JJ012 cells, whereas panel B demonstrates one of the 10 representative experiments of the PRP-1 treated JJ012 cells. These were performed to demonstrate how the gating was performed by the flow cytometry software. (C) Histogram of the mean percentages of cells in PRP-1-treated and untreated fractions (n=10). (D) Trypan blue staining of ALDH fractions and JJ012 untreated controls. (E) Histogram of the viability in ALDH-treated and untreated fractions and JJ012 control cells. (F) Western blot of ALDH1A1 expression in $ALDH^{high\text{-}untreated}$ and $ALDH^{low\text{-}PRP\text{-}1}$. (G) Histogram of relative OD in $ALDH^{high\text{-}untreated}$ and $ALDH^{low\text{-}PRP\text{-}1}$. $^{*}P<0.05$, $^{**}P<0.01$ and $^{***}P<0.001$. ALDH, aldehyde dehydrogenase; OD, optical density; PRP-1, proline-rich polypeptide-1.

PRP-1-treated JJ012 ($ALDH^{high\text{-}PRP\text{-}1}$) were difficult to collect as a result of the exceedingly low levels of these CSC populations following treatment with PRP-1; however, this was eventually accomplished following multiple experiments and compilation of the sorting results (Table SII).

The cell viability assay demonstrated an increase in non-viable cells in the PRP-1 treated cells compared with the untreated cells (Fig. 2D; Tables SIII and SIV). One-way ANOVA analysis demonstrated significant differences amongst the controls and subpopulations following 72 h PRP-1

treatment between the JJ012 control and PRP-1 treated JJ012 (Tables SIII and SIV; Fig. 1E).

Following subpopulation collection and cell lysis, western blot analysis demonstrated a significant decrease of ALDH1A1 protein expression between subpopulations with and without PRP-1 treatment (Fig. 2F). Densitometry analysis demonstrated a statistically significant difference in ALDH1A1 protein expression between $ALDH^{high\text{-}untreated}$ cells vs. $ALDH^{low\text{-}PRP\text{-}1}$ cells. When comparing the mean relative OD of ALDH between $ALDH^{high\text{-}untreated}$ (mean OD, 3.590±0.040; n=2) and $ALDH^{low\text{-}PRP\text{-}1}$ (mean OD, 1.224±0.009; n=2) cells, Student's t-test demonstrated a significant 2.93-fold decrease in ALDH expression in $ALDH^{low\text{-}PRP\text{-}1}$ cells [t(2)=57.23; P=0.0003; Fig. 2G; Table SV].

Epigenetic mechanism of CSC regulation by PRP-1 in chondrosarcoma JJ012 cell line. The epigenetic effect of PRP-1 on CSCs was assessed. In order to further elucidate the molecular mechanism by which PRP-1 decreases CSC-population, the effect of PRP-1 on important epigenetic readers, such as the BD and BET proteins (26). TOP2A is an important enzyme in the regulation of DNA structure and cell proliferation (27-31). However, the results of the present study failed to demonstrate downregulation of TOP2A activity following treatment with PRP-1 (data not shown).

Comparison of BAF170 expression between $ALDH^{high\text{-}untreated}$ and $ALDH^{low\text{-}PRP\text{-}1}$ cells demonstrated a significant decrease in the mean relative OD in $ALDH^{low\text{-}PRP\text{-}1}$ cells (Fig. 3). In addition, BRG1 expression was significantly decreased in $ALDH^{low\text{-}PRP\text{-}1}$ cells compared with that in $ALDH^{high\text{-}untreated}$ cells. $ALDH^{low\text{-}PRP\text{-}1}$ cells demonstrated a significant decrease in BRM expression compared with $ALDH^{high\text{-}untreated}$ cells (Table SVI). No differences were observed between fractions with or without PRP-1 treatment for BAF155 or STRO-1 mesenchymal stem cell factor (Fig. 3A). The downstream targets for BMI-1, such as p14 ARF and p15/p16 did not exhibit any changes at the protein level (Fig. 3B), which suggested that the oncogenic function of BMI-1 in chondrosarcoma was independent from these downstream targets.

Discussion

The aforementioned conventional and mesenchymal stem cell markers CD144, CD117, CD221, LGR5, CD271, CD10, BMI, FOXC1 and c-Myc are notable in bone sarcoma stem cells; however, there is no definitive marker for bone chondrosarcoma stem cells other than ALDH1A1 (16). The present study aimed to identify novel specific markers for chondrosarcoma stem cells. The results demonstrated that none of the known markers for other types of sarcoma were identified as chondrosarcoma biomarkers. Thus, the search for potential epigenetic players that decrease the CSC population following PRP-1 treatment remains critical. A previous study has reported that PRP-1 attenuates miR-302 (part of miR-302-367 cluster) expression and targets the embryonic stem cell markers Nanog, polycomb protein BMI-1 and c-Myc (2). A previous study on PRP-1 in the human chondrosarcoma JJ012 cell line investigated the effect of peptides on JJ012 subpopulations, and the outcome indicated that PRP-1 treatment notably decreased $ALDH^{high}$ cells from bulk JJ012 population (25).

In the present study, low activity of embryonic stem cell markers was observed in chondrosarcoma JJ012 cells treated with PRP-1, which were identified as $ALDH^{low\text{-}PRP\text{-}1\text{-}treated}$ following sorting.

The oncogene *BMI-1 is* a member of the polycomb-group family of proteins, and is frequently overexpressed in different types of tumor to promote carcinogenesis and drive stem cell-like properties (32-43). BMI-1 knockdown using RNA interference was demonstrated to significantly impair osteosarcoma cell viability, *in vitro* colony formation and *in vivo* tumorigenesis, as well as to sensitize osteosarcoma cells to cisplatin-induced apoptosis (41). BMI-1 targets Ink4a/ARF, which encodes vital cell cycle inhibitors such as the human product of CDKN2A gene p16 (Ink4a) (17), which helps regulate stem cells. BMI-1 represses the *Ink4a/ARF* locus and the onset of senescence in human embryonic fibroblasts (43). However, the inhibitory effect of PRP-1 on BMI-1 was demonstrated to be independent of *Ink4a/ARF* at the protein levels in the present study, as no difference in protein expression was observed with or without PRP-1 treatment.

As PRP-1 has been demonstrated to inhibit Nanog (1), the present study assessed its upstream regulator, BRD4, which is a member of the bromodomain (BD) and extraterminal domain (BET), an important hallmark of cancer and epigenetic regulation and marker for stem cell self-renewal (44). BRD4 binds to acetylated histones at enhancers and promoters via its BDs in order to regulate transcriptional elongation and gene expression programs that have pivotal roles in inflammation and cancer development (44-47). BRD4 JQ1, a BET inhibitor, suppresses c-Myc and inhibits cell proliferation, and induces cell senescence and apoptosis in human chondrosarcoma cells (48). The cytostatic effect of PRP-1 has been demonstrated to be mediated by c-Myc inhibition in human chondrosarcoma cells (11). Over the past decade, the BD, BRD4, BET proteins have emerged as an important class of epigenetic readers (27). However, PRP-1 did not act an inhibitor of BRD4 in the present study.

TOP2A is an important enzyme in the regulation of DNA structure and cell proliferation (28-31). High TOP2A expression has been reported in advanced leiomyosarcoma, high mitotic index and advanced stage tumors (31). TOP2A is highly expressed in soft tissue sarcomas and is an independent predictor of poor prognosis (30). However, the results of the present study failed to demonstrate downregulation of TOP2A activity following treatment with PRP-1.

Gene transcription is dynamically regulated in stemness and cell proliferation (34,35). The chromatin remodeling complexes can affect whether a gene is activated or repressed, therefore the effect of PRP-1 on SWI/SNF remodeling complexes was assessed, which depends on ATP as its energy source, and its subunits BAF170 (SMARCC2), BAF155 (SMARCC1) and BRG1 (SMARCA4) (49-52). The mammalian SWI/SNF-like ATP-dependent chromatin remodeling complex, also termed BAF/BRG/Brahma associated (esBAF) can either activate or repress transcription (51). These factors are recruited by transcription factors to the promoters of target genes, where they can disrupt histone-DNA contacts and allow transcription factors to access their sequence-specific DNA (52). Depending on whether a transcriptional activator or repressor recruits SWI/SNF, transcription can be

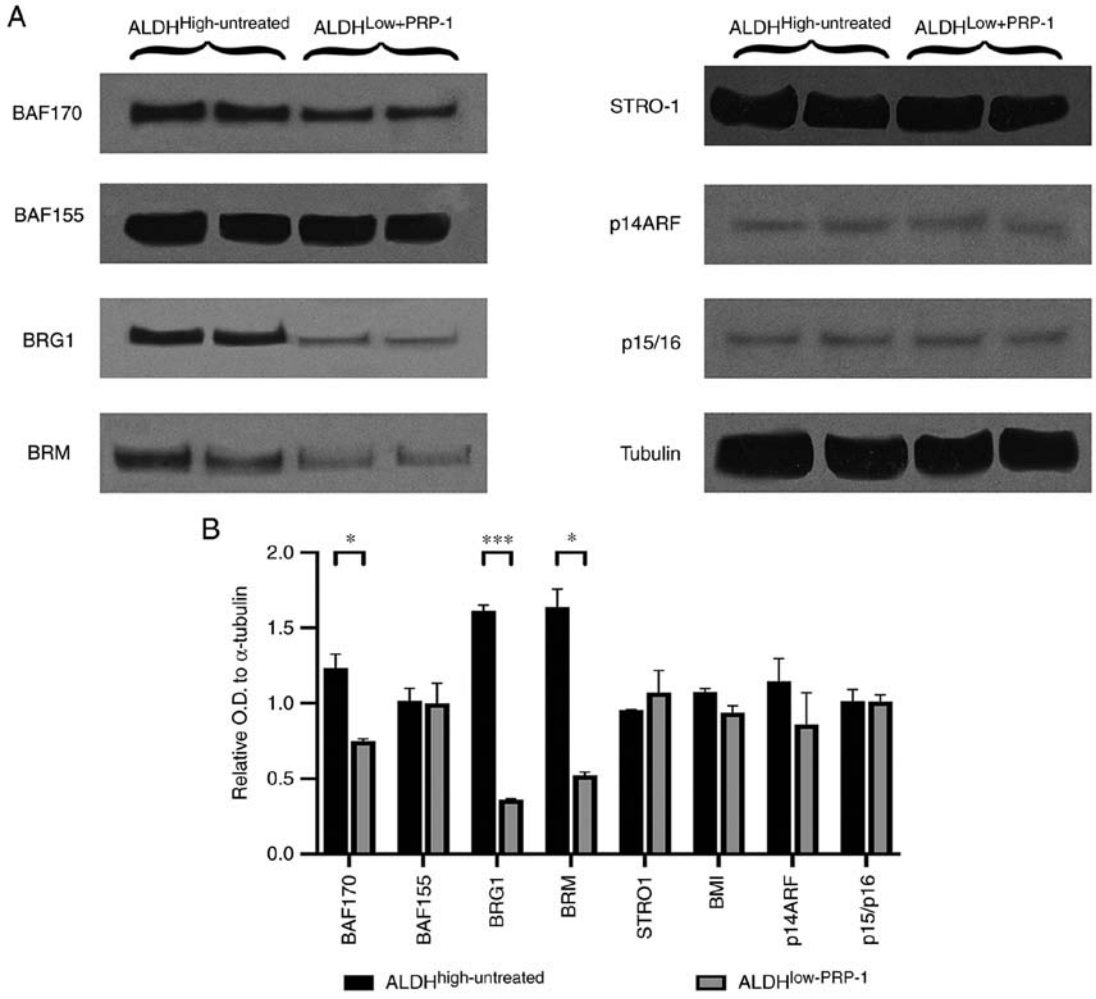

Figure 3. (A) Western blot analysis of Switch/sucrose non-fermenting complex key components in ALDH$^{high\text{-}untreated}$ and ALDH$^{low\text{-}PRP\text{-}1}$ fractions. PRP-1 induced decreases in the protein expression of BAF 155, BRG 1 and BAF170 in ALDH$^{low\text{-}PRP\text{-}1}$ fractions compared with that in ALDH$^{high\text{-}untreated}$ fractions. Mesenchymal stem cell factor STRO-1 protein levels were not different between the fractions and were not affected by PRP-1. BMI-1 oncogene targets p14ARF, and p15/p16 displayed the same protein levels, and PRP-1 did not cause any changes. (B) Histograms of the relative OD in the western blots. *P<0.05, **P<0.01 and ***P<0.001. ALDH, aldehyde dehydrogenase; OD, optical density; PRP-1, proline-rich polypeptide-1; BRG1, protein Brahma homolog 1; BAF 170, BRM BRG1-associated factor 170; BAF 155, BRG1-associated factor155; BMR, bromodomain protein; p14ARF, ARF tumor suppressor; p15/p16, cyclin-ependent kinase inhibitor 2A.

upregulated or downregulated accordingly (52). The energy from ATP hydrolysis is harnessed to disrupt histone-DNA contacts and move nucleosomes away from the transcription start site or towards it (52). Specifically, alterations to mammalian SWI/SNF (mSWI/SNF or BAF) ATP-dependent chromatin remodeling complexes and polycomb repressive complexes cause disease-specific changes in the chromatin architecture and gene expression across a number of sarcoma subtypes such as Ewing's, synovial sarcoma and chondrosarcoma (48). SWI/SNF is essential for self-renewal of stem cells and is critical for cell differentiation (49). A previous study on chondrosarcoma reported that poorly differentiated types of tumor were demonstrated to exhibit similarities with mesenchymal stem cells at pre-chondrogenic stages, whereas more differentiated types of tumor shared similarities with fully differentiated chondrocytes (53). This suggested that chondrosarcoma progression may be parallel to the deregulated chondrocyte differentiation process of MSCs (53). Future studies will investigate whether the inhibitory effect of PRP-1 on CSC leads to the revival of the differentiation program.

Well-established interactions between esBAF and polycomb complexes have been documented, which can act antagonistically () or synergistically cooperate with polycomb group proteins to support pluripotency (54,55). BRG1 and BRM have the ability to act as either oncogenes or tumor suppressors (54). The results of the present study demonstrated that inhibition of BMI-1 with PRP-1 was accompanied by inhibition of both subunits of the esBAF complex (BRG1 and BRM), which possess oncogenic properties in chondrosarcoma. Depletion of BAF170 (SMARCC2) instead of BAF155 (SMARCC1) resulted in the loss of stem cell properties in hESCs, and this pattern was different from that observed in rodent stem cells (i.e., mESCs and mEpiSCs) (55-58). Deletion of *BRG1* (SMARCA4) in embryonic stem cells results in the loss of both self-renewal capacity and pluripotency (57). In the present study, BAF 155 was not affected by PRP-1 treatment, whereas BAF170 protein expression, BRM and BRG1 were all demonstrated to be inhibited following treatment compared with untreated cells Genome-wide studies have indicated that BRG1 and BRM have cooperative and antagonistic interactions in transcription (36). The results of

the present study demonstrated that downregulation of BAF 170, BRG and BRM by PRP-1 may act in favor of synergistic regulation of BRG and BRM in chondrosarcoma, and that they may possess oncogenic properties in this microenvironment.

Cytostatic drugs can lead to decreased cell viability (12-14). Autophagy is a tightly regulated catabolic process of cellular self-digestion by which cellular components are targeted to lysosomes for their degradation (59). The present study failed to detect any apoptotic action of PRP-1 (data not shown). In cell cultures, certain drugs that activate autophagy have been associated with programmed cell death, but not apoptosis. Autophagy has been demonstrated to be essential for cell death, especially in cell lines that are resistant to apoptosis-driven chemotherapy, which may benefit from directly destroying tumor cells or sensitizing them to chemotherapy (59,60). Thus, it may be assumed that drastic elimination of chondrosarcoma stem cells by PRP-1 may be mediated by targeting BAF chromatin remodeling complexes and by induction of autophagy. A potential future study will aim to investigate whether this inhibition serves a pivotal role in the process of cancer stem cell decrease mediated by the peptide action.

In conclusion, the results of the present study demonstrated that ALDH1A1 is the only current biomarker in chondrosarcoma CSCs. PRP-1 decreased CSCs across all experiments. As a possible mechanismthe results of the present study indicated that PRP-1 may target chromatin remodeling complexes. Our future efforts will be directed towards understanding the interconnection between CSC maintenance, self-renewal and BAF complexes.

Acknowledgements

The authors would like to thank Patricia Lissette Guevara, M.A from the Flow Cytometry Core Facility, Miller School of Medicine for her assistance in data acquisition, and analysis. The authors would also like to thank Dr Joel Block's Laboratory (Rush University, Chicago, USA) for providing the human JJ012 chondrosarcoma cells; Dr Messner (Ontario Cancer Institute, Canada) for Ly10 cells; and Dr Vega (MD Anderson Cancer Center, Houston, TX, USA) for HBL-1 cells. PRP-1 was provided by professor A. Galoyans laboratory H, Buniatian Institute of Biochemistry of National Academy of Sciences of Armenia. The authors would also like to thank Dr Claude Henry Volmar, Director of the Research Laboratory for the Center of Therapeutic Innovation, University of Miami, Miller School of Medicine for assisting with BRD4 experiments.

Funding

The present study was supported in part by the Ratcliffe Foundation to Miami Center of Orthopaedic Research and Education and the Department of Orthopedics, University of Miami, Miller School of Medicine.

Availability of data and materials

All data generated or analyzed during this study are included in this published article

Authors' contributions

AM conducted most of the experiments and was involved in manuscript writing. AH and AS performed western blot experiments, statistical and image analysis. CG participated in data analysis and certain experiments. SS performed fluorescence-activated cell sorting and flow cytometry data analysis. MB performed lymphoma cell line experiments with PRP-1 and participated in the critical revision of this manuscript. LZJ tested the PRP-1 action in melanoma cell line and contributed to the acquisition, analysis and interpretation of the data. SAC and JP provided substantial contributions to the conception and design and participated in critical revision of the manuscript. JB performed western blotting experiments. KG designed the study, wrote parts of the manuscript and was involved in the critical revision of it. All authors have read and approved the final manuscript.

Ethics approval and consent to participate

Not applicable.

Patient consent for publication

Not applicable.

Competing interests

The authors declare that they have no competing interests.

References

1. Dorfman HD and Czerniak B: Bone cancers. Cancer 75 (1 Suppl): S203-S210, 1995.
2. Fujiwara T and Ozaki T: Overcoming therapeutic resistance of bone sarcomas: Overview of the molecular mechanisms and therapeutic targets for bone sarcoma stem cells. Stem Cells Int 2016: 2603092, 2016.
3. Galoian K, Qureshi A, D'Ippolito G, Schiller PC, Molinari M, Johnstone AL, Brothers SP, Paz AC and Temple HT: Epigenetic regulation of embryonic stem cell marker miR302C in human chondrosarcoma as determinant of antiproliferative activity of proline-rich polypeptide 1. Int J Oncol 47: 465-472, 2015.
4. Galoian K, Abrahamyan S, Chailyan G, Qureshi A, Patel P, Metser G, Moran A, Sahakyan I, Tumasyan N, Lee A, *et al*: Toll like receptors TLR1/2, TLR6 and MUC5B as binding interaction partners with cytostatic proline rich polypeptide 1 in human chondrosarcoma. Int J Oncol 52: 139-154, 2018.
5. Vermeulen L, Todaro M, de Sousa Mello F, Sprick MR, Kemper K, Perez Alea M, Richel DJ, Stassi G and Medema JP: Single-cell cloning of colon cancer stem cells reveals a multi-lineage differentiation capacity. Proc Natl Acad Sci USA 105: 13427-13432, 2008.
6. Sell S: On the stem cell origin of cancer. Am J Pathol 176: 2584-2494, 2010.
7. Honoki K, Fujii H, Kubo A, Kido A, Mori T, Tanaka Y and Tsujiuchi T: Possible involvement of stem-like populations with elevated ALDH1 in sarcomas for chemotherapeutic drug resistance. Oncol Rep 24: 501-505, 2010.
8. Tanei T, Morimoto K, Shimazu K, Kim SJ, Tanji Y, Taguchi T, Tamaki Y and Noguchi S: Association of breast cancer stem cells identified by aldehyde dehydrogenase 1 expression with resistance to sequential paclitaxel and epirubicin-based chemotherapy for breast cancers. Clin Cancer Res 15: 4234-4241, 2009.
9. Awad O, Yustein JT, Shah P, Gul N, Katuri V, O'Neill A, Kong Y, Brown ML, Toretsky JA and Loeb DM: High ALDH activity identifies chemotherapy-resistant Ewing's sarcoma stem cells that retain sensitivity to EWS-FLI1 inhibition. PLoS One 5: e13943, 2010.

10. Galoyan A: Neurochemistry of brain neuroendocrine immune system: Signal molecules. Neurochem Res 25: 1343-1355, 2000.
11. Galoian K, Temple TH and Galoyan A: Cytostatic effect of the hypothalamic cytokine PRP-1 is mediated by mTOR and cMyc inhibition in high grade chondrosarcoma. Neurochem Res 36: 812-818, 2011.
12. Galoian K, Qureshi A, Wideroff G and Temple HT: Restoration of desmosomal junction protein expression and inhibition of H3K9-specific histone demethylase activity by cytostatic proline-rich polypeptide-1 leads to suppression of tumorigenic potential in human chondrosarcoma cells. Mol Clin Oncol 3: 171-178, 2015.
13. Galoian K, Luo S, Qureshi A, Patel P, Price R, Morse AS, Chailyan G, Abrahamyan S and Temple HT: Effect of cytostatic proline rich polypeptide-1 on tumor suppressors of inflammation pathway signaling in chondrosarcoma. Mol Clin Oncol 5: 618-624, 2016.
14. Galoian KA, Guettouche T, Issac B, Qureshi A and Temple HT: Regulation of onco and tumor suppressor MiRNAs by mTORC1 inhibitor PRP-1 in human chondrosarcoma. Tumour Biol 35: 2335-2341, 2014.
15. Galoian KA, Temple TH and Galoyan A: Cytostatic effect of novel mTOR inhibitor, PRP-1 (galarmin) in MDA 231 (ER-) breast carcinoma cell line. PRP-1 inhibits mesenchymal tumors. Tumour Biol 32: 745-751, 2011.
16. Lohberger B, Rinner B, Stuendl N, Absenger M, Liegl-Atzwanger B, Walzer SM, Windhager R and Leithner A: Aldehyde dehydrogenase 1, a potential marker for cancer stem cells in human sarcoma. PLoS One 7: e43664, 2012.
17. Ginestier C, Hur MH, Charafe-Jauffret E, Monville F, Dutcher J, Brown M, Jacquemier J, Viens P, Kleer CG, Liu S, *et al*: ALDH1 is a marker of normal and malignant human mammary stem cells and a predictor of poor clinical outcome. Cell Stem Cell 1: 555-567, 2007.
18. Nakahata K, Uehara S, Nishikawa S, Kawatsu M, Zenitani M, Oue T and Okuyama H: Aldehyde dehydrogenase 1 (ALDH1) is a potential marker for cancer stem cells in embryonal rhabdomyosarcoma. PLoS One 10: e0125454, 2015.
19. Tolstorukov MY, Sansam CG, Lu P, Koellhoffer EC, Helming KC, Alver BH, Tillman EJ, Evans JA, Wilson BG, Park PJ and Roberts CW: Swi/Snf chromatin remodeling/tumor suppressor complex establishes nucleosome occupancy at target promoters. Proc Natl Acad Sci USA 110: 10165-10170, 2013.
20. Ueda K, Ogasawara S, Akiba J, Nakayama M, Todoroki K, Ueda K, Sanada S, Suekane S, Noguchi M, Matsuoka K and Yano H: Aldehyde dehydrogenase 1 identifies cells with cancer stem cell-like properties in a human renal cell carcinoma cell line. PLoS One 8: e75463, 2013.
21. Hoyt AK, Moran A, Granger C, Sedani A, Saigh S, Brown J and Galoian KA: PRP1 significantly decreases the ALDHhigh cancer stem cell population and regulates the aberrant Wnt/β-catenin pathway in human chondrosarcoma JJ012 cells. Oncol Rep 42: 103-114, 2019.
22. Kim WT and Ryu CJ: Cancer stem cell surface markers on normal stem cells. BMB Rep 50: 285-298, 2017.
23. Wirths S, Malenke E, Kluba T, Rieger S, Müller MR, Schleicher S, Hann von Weyhern C, Nagl F, Fend F, Vogel W, *et al*: Shared cell surface marker expression in mesenchymal stem cells and adult sarcomas. Stem Cells Transl Med 2: 53-60, 2013.
24. Genadry KC, Pietrobono S, Rota R and Linardic CM: Soft tissue sarcoma cancer stem cells: An overview. Front Oncol 8: 475, 2018.
25. Mak AB, Pehar M, Nixon AM, Williams RA, Uetrecht AC, Puglielli L and Moffat J: Post-translational regulation of CD133 by ATase1/ATase2-mediated lysine acetylation. J Mol Biol 426: 2175-2182, 2014.
26. Jacques C, Lamoureux F, Baud'huin M, Rodriguez Calleja L, Quillard T, Amiaud J, Tirode F, Rédini F, Bradner JE, Heymann D and Ory B: Targeting the epigenetic readers in Ewing sarcoma inhibits the oncogenic transcription factor EWS/Fli1. Oncotarget 7: 24125-24140, 2016.
27. Wang JC: Cellular roles of DNA topoisomerases: A molecular perspective. Nat Rev Mol Cell Biol 3: 430-440, 2002.
28. Pulleyblank DE: Of topo and maxwell's dream. Science 277: 648-649, 1997.
29. Li TK and Liu LF: Tumor cell death induced by topoisomerase-targeting drugs. Annu Rev Pharmacol Toxicol 41: 53-77, 2001.
30. da Cunha IW, De Brot L, Carvalho KC, Rocha RM, Fregnani JH, Falzoni R, Ferreira Fde O, Aguiar S Jr, Lopes A, Muto NH, *et al*: Prognostication of soft tissue sarcomas based on chromosome 17q gene and protein status: Evaluation of TOP2A, HER-2/neu, and survivin. Ann Surg Oncol 19: 1790-1799, 2012.
31. Baiocchi G, Poliseli FL, De Brot L, Mantoan H, Schiavon BN, Faloppa CC, Vassallo J, Soares FA and Cunha IW: TOP2A copy number and TOP2A expression in uterine benign smooth muscle tumours and leiomyosarcoma. J Clin Pathol 69: 884-889, 2016.
32. Raab JR, Runge JS, Spear CC and Magnuson T: Co-regulation of transcription by BRG1 and BRM, two mutually exclusive SWI/SNF ATPase subunits. Epigenetics Chromatin 10: 62, 2017.
33. Douglas D, Hsu JH, Hung L, Cooper A, Abdueva D, van Doorninck J, Peng G, Shimada H, Triche TJ and Lawlor ER: BMI-1 promotes ewing sarcoma tumorigenicity independent of CDKN2A repression. Cancer Res 68: 6507-6515, 2008.
34. Pietersen AM, Horlings HM, Hauptmann M, Langerød A, Ajouaou A, Cornelissen-Steijger P, Wessels LF, Jonkers J, van de Vijver MJ and van Lohuizen M: EZH2 and BMI1 inversely correlate with prognosis and TP53 mutation in breast cancer. Breast Cancer Res 10: R109, 2008.
35. Dhawan S, Tschen SI and Bhushan A: Bmi-1 regulates the Ink4a/Arf locus to control pancreatic beta-cell proliferation. Genes Dev 23: 906-911, 2009.
36. Becker M, Korn C, Sienerth AR, Voswinckel R, Luetkenhaus K, Ceteci F and Rapp UR: Polycomb group protein Bmi1 is required for growth of RAF driven non-small-cell lung cancer. PLoS One 4: e4230, 2009.
37. Dovey JS, Zacharek SJ, Kim CF and Lees JA: Bmi1 is critical for lung tumorigenesis and bronchioalveolar stem cell expansion. Proc Natl Acad Sci USA 105: 11857-11862, 2008.
38. Bruggeman SW, Hulsman D, Tanger E, Buckle T, Blom M, Zevenhoven J, van Tellingen O and van Lohuizen M: Bmi1 controls tumor development in an Ink4a/Arf-independent manner in a mouse model for glioma. Cancer Cell 12: 328-341, 2007.
39. Wang E, Bhattacharyya S, Szabolcs A, Rodriguez-Aguayo C, Jennings NB, Lopez-Berestein G, Mukherjee P, Sood AK and Bhattacharya R: Enhancing chemotherapy response with Bmi-1 silencing in ovarian cancer. PLoS One 6: e17918, 2011.
40. Hsu JH and Lawlor ER: BMI 1 suppresses contact inhibition and stabilizes YAP in Ewing sarcoma. Oncogene 30: 2077-2085, 2011.
41. Wu Z, Min L, Chen D, Hao D, Duan Y, Qiu G and Wang Y: Overexpression of BMI-1 promotes cell growth and resistance to cisplatin treatment in osteosarcoma. PLoS One 6: e14648, 2011.
42. Liu L, Andrews LG and Tollefsbol TO: Loss of the human polycomb group protein BMI1 promotes cancer-specific cell death. Oncogene 25: 4370-4375, 2006.
43. Bracken AP, Kleine-Kohlbrecher D, Dietrich N, Pasini D, Gargiulo G, Beekman C, Theilgaard-Mönch K, Minucci S, Porse BT, Marine JC, *et al*: The Polycomb group proteins bind throughout the INK4A-ARF locus and are disassociated in senescent cells. Genes Dev 21: 525-530, 2007.
44. Liu W, Stein P, Cheng X, Yang W, Shao NY, Morrisey EE, Schultz RM and You J: BRD4 regulates Nanog expression in mouse embryonic stem cells and preimplantation embryos. Cell Death Differ 21: 1950-1960, 2014.
45. Gonzales-Cope M, Sidoli S, Bhanu NV, Won KJ and Garcia BA: Histone H4 acetylation and the epigenetic reader Brd4 are critical regulators of pluripotency in embryonic stem cells. BMC Genomics 17: 95, 2016.
46. Rahnamoun H, Lee J, Sun Z, Lu H, Ramsey KM, Komives EA and Lauberth SM: RNAs interact with BRD4 to promote enhanced chromatin engagement and transcription activation. Nat Struct Mol Biol 25: 687-697, 2018.
47. Zhang HT, Gui T, Sang Y, Yang J, Li YH, Liang GH, Li T, He QY and Zha ZG: The BET bromodomain inhibitor JQ1 suppresses chondrosarcoma cell growth via regulation of YAP/p21/c-Myc signaling. J Cell Biochem 118: 2182-2192, 2017.
48. McBride MJ and Kadoch C: Disruption of mammalian SWI/SNF and polycomb complexes in human sarcomas: Mechanisms and therapeutic opportunities. J Pathol 244: 638-649, 2018.
49. De-Meng Chen X-QZ, Kai Wang and Yi-Zhou Jiang: SWI/SNF chromatin remodeling complex in regulating mesenchymal stem cell lineage specification. J Tissue Sci Engineering 6: 154, 2015.
50. Yang J, Ren Z, Du X, Hao M and Zhou W: The role of mesenchymal stem/progenitor cells in sarcoma: Update and dispute. Stem Cell Investig 1: 18, 2014.

51. Tang L, Nogales E and Ciferri C: Structure and function of SWI/SNF chromatin remodeling complexes and mechanistic implications for transcription. Prog Biophys Mol Biol 102: 122-128, 2010.
52. Wilson BG, Wang X, Shen X, McKenna ES, Lemieux ME, Cho YJ, Koellhoffer EC, Pomeroy SL, Orkin SH and Roberts CW: Epigenetic antagonism between polycomb and SWI/SNF complexes during oncogenic transformation. Cancer Cell 18: 316-328, 2010.
53. de Andrea CE and Hogendoorn PC: Epiphyseal growth plate and secondary peripheral chondrosarcoma: The neighbours matter. J Pathol 226: 219-228, 2012.
54. Kadoch C, Williams RT, Calarco JP, Miller EL, Weber CM, Braun SM, Pulice JL, Chory EJ and Crabtree GR: Dynamics of BAF-Polycomb complex opposition on heterochromatin in normal and oncogenic states. Nat Genet 49: 213-222, 2017.
55. Shao Z, Raible F, Mollaaghababa R, Guyon JR, Wu CT, Bender W and Kingston RE: Stabilization of chromatin structure by PRC1, a Polycomb complex. Cell 98: 37-46, 1999.
56. Poynter ST and Kadoch C: Polycomb and trithorax opposition in development and disease. Wiley Interdiscip Rev Dev Biol 5: 659-688, 2016.
57. Zhang X, Li B, Li W, Ma L, Zheng D, Li L, Yang W, Chu M, Chen W, Mailman RB, *et al*: Transcriptional repression by the BRG1-SWI/SNF complex affects the pluripotency of human embryonic stem cells. Stem Cell Reports 3: 460-474, 2014.
58. Kahali B, Yu J, Marquez SB, Thompson KW, Liang SY, Lu L and Reisman D: The silencing of the SWI/SNF subunit and anti-cancer gene BRM in Rhabdoid tumors. Oncotarget 5: 3316-3332, 2014.
59. Fulda S and Kogel D: Cell death by autophagy: Emerging molecular mechanisms and implications for cancer therapy. Oncogene 34: 5105-5113, 2015.
60. Kanzawa T, Germano IM, Komata T, Ito H, Kondo Y and Kondo S: Role of autophagy in temozolomide-induced cytotoxicity for malignant glioma cells. Cell Death Differ 11: 448-457, 2004.